CERIAS Tech Report 2006-46

A Reliability Engineering Approach to Digital Watermark Evaluation

by Hyung Cook Kim and Edward J. Delp

Center for Education and Research in
Information Assurance and Security,
Purdue University, West Lafayette, IN 47907-2086

A Reliability Engineering Approach to Digital Watermark Evaluation

Hyung Cook Kim and Edward J. Delp

Video and Image Processing Laboratory (VIPER)
School of Electrical and Computer Engineering
Purdue University
West Lafayette, Indiana USA

ABSTRACT

Robust watermarks are evaluated in terms of image fidelity and robustness. We extend this framework and apply reliability testing to robust watermark evaluation. Reliability is the probability that a watermarking algorithm will correctly detect or decode a watermark for a specified fidelity requirement under a given set of attacks and images. In reliability testing, a system is evaluated in terms of quality, load, capacity and performance. To measure quality that corresponds to image fidelity, we compensate for attacks to measure the fidelity of attacked watermarked images. We use the conditional mean of pixel values to compensate for valumetric attacks such as gamma correction and histogram equalization. To compensate for geometrical attacks, we use error concealment and perfect motion estimation assumption. We define capacity to be the maximum embedding strength parameter and the maximum data payload. Load is then defined to be the actual embedding strength and data payload of a watermark. To measure performance, we use bit error rate (BER) and receiver operating characteristics (ROC) and area under the curve (AUC) of the ROC curve of a watermarking algorithm for different attacks and images. We evaluate robust watermarks for various quality, loads, attacks, and images.

Keywords: Digital Watermarking, Robust Still Image Watermark Evaluation, Compensated Mean Square Error, Reliability Testing

1. INTRODUCTION

Robust image watermarks are image watermarks designed to survive attacks that include signal processing and spatial transformations [1–3]. As recognized in [4], we need fair watermark evaluation methods and benchmarks to facilitate the advancement of robust digital watermarking. Because of this need, various evaluation methods and benchmarks have been developed [4–14]. A block diagram of a typical robust watermarking model [15] is shown in Figure 1. Important properties of robust watermarks are fidelity and performance of the watermark against different attacks [1]. Fidelity is the perceptual similarity between the original and watermarked image. Performance is the ability to detect/decode the watermark. Attacks are important part of watermark evaluation and various attacks are implemented as part of benchmarks [6–8]. We use StirMark 4.0 [6, 7] attacks in this paper. There is a trade off between performance and fidelity [4] and we control this trade off by using the embedding strength α shown in Figure 1. The most popular fidelity measure for images is the mean square error (MSE) [16] and PSNR which is a logarithmic scaled MSE [16]. Because PSNR [16] does not correlate too well with the human visual system (HVS), other more sophisticated objective fidelity metrics have been used for watermark evaluation [4, 5, 8, 12, 14]. For performance measures, receiver operating characteristic (ROC), bit error rate (BER), and message error rate are generally used [1, 4, 17]. To display evaluation results, the use of "BER versus visual quality," "BER versus attack," "attack versus visual quality" for a fixed BER, was proposed in [4]. In watermark evaluation, it is important to summarize the results to facilitate the comparison of algorithms. For BER, the results are summarized using message error rate or average bit error rate [4]. For fidelity metric summarization, some iterate the embedding strength for each image to meet a fidelity requirement

This work was supported by the Air Force Research Laboratory, Information Directorate, Rome Research Site, under research grant number F30602-02-2-0199. Address all correspondence to E. J. Delp, ace@ecn.purdue.edu.

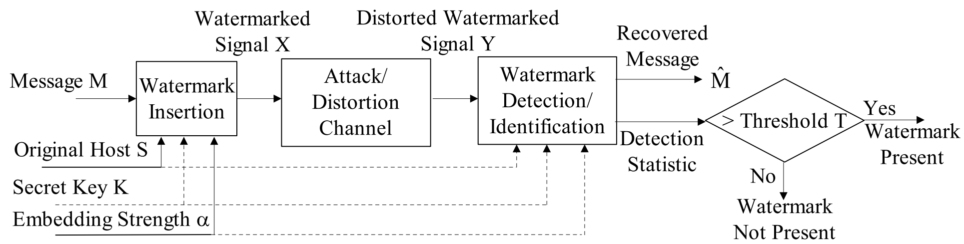

Figure 1. A Block Diagram of a Watermarking System [15]

threshold [4, 5, 11, 12]. To summarize ROC, area under the curve (AUC), equal error rate, false negative rate for a fixed false positive probability are used [4, 11].

Many of the watermark evaluation methods fit into the reliability testing framework [18]. We define reliability as the probability that a watermarking algorithm will correctly detect or decode a watermark for a specified fidelity requirement under a given set of attacks and images. In reliability testing, a system is evaluated in terms of quality, load, capacity, and performance. To measure quality that corresponds to image fidelity, we need to measure the fidelity of the attacked image as well as the watermarked image. PSNR, as it is, cannot be used to measure fidelity for valumetric attacks [1, 19] such as gamma correction or amplitude scaling, pixel loss attacks such as cropping or random row column removal [4, 6, 7], geometrical attacks such as image shifting or aspect ratio change. In this paper, we will measure fidelity of these attacks by compensating the attacks [12]. Using this new measure, we will evaluate watermark algorithms in a reliability testing framework by varying embedding strength, payload and measure the performance and fidelity. This paper is organized as follows: In section 2, we describe a technique to measure fidelity in terms of mean square error for valumetric attacks, pixel loss attacks, and geometrical attacks. In section 3, we define quality, load, capacity, and performance and evaluate watermarking algorithms by varying quality and load. The conclusion and future work is given in section 4.

2. COMPENSATED MEAN SQUARE ERROR

Measuring fidelity of the attacked images is important as well as measuring the fidelity of the watermarked image. In [12], fidelity evaluation for geometrical attacks are given. In [14], conditional entropy is used to evaluate valumetric attacks including histogram equalization, and amplitude scaling. In the following, we will extend MSE by compensating for valumetric attacks, geometrical attacks, and pixel loss attacks. A distortion function we will use is given below and similar to the one given in [20].

$$d(\mathbf{s}, \mathbf{y}) = \min_{\theta \in \Theta} \|\mathbf{s} - T_\theta \mathbf{y}\|^2$$

, where Θ is the set of compensating functions. We develop T_θ for geometrical attacks, valumetric attacks and pixel loss attacks and combine them to measure in terms of MSE. For test images, we will use the images shown in Figure 2.

2.1. Compensation for Valumetric Attacks

Valumetric Attacks or point operations are zero memory operations where a function $f(s)$ maps a pixel value s to $f(y)$ [16, 19]. Valumetric attacks include contrast stretching, digital negative, range compression, and histogram equalization. These point operation functions are either monotonically increasing or decreasing. We assume that these operations work because HVS determines the content not by the exact value of a pixel but the rank of the pixel values. This is analogous to changing keys in music.

Let $\hat{s}(y)$ be a function that maps the attacked image pixel values to other pixel values. This function is defined only for values y such that $p(y) > 0$. We can write MSE for the image produced by the mapping $\hat{s}(y)$ using the joint probability as follows:

$$MSE(s, y) = \sum_{s} \sum_{y, p(y)>0} (s - \hat{s}(y))^2 p(s, y).$$

(a) fcc-door(440x324)

(b) 0115(600x400)

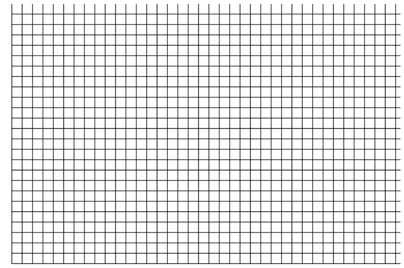

(c) grid-16-16(600x400)

Figure 2. Test Images.

It is well known that $\hat{s}_{mmse}(y)$ $(p(y) > 0)$, which minimizes MSE, is the conditional mean,

$$\hat{s}_{mmse}(y) = \sum_s sp(s|y).$$

THEOREM 2.1. *Let $y = f(s)$ be a monotonically increasing function. Then $\hat{s}_{mmse}(y)$ is an increasing function for values of y s.t. $p(y) > 0$.*

Proof.

We can rewrite $\hat{s}_{mmse}(y)$ as follows:

$$\hat{s}_{mmse}(y) = \sum_{s,p(s)>0,f(s)=y} sp(s|y).$$

Because $\sum_s p(s|y) = 1$, $\hat{s}_{mmse}(y)$ is an weighted average of s's for $f(s) = y$. By the definition of f, if s_1 and s_2 exists s.t. $f(s_1) > f(s_2)$ then $s_1 > s_2$. This implies that if $y_1 > y_2$, then $\hat{s}_{mmse}(y_1) > \hat{s}_{mmse}(y_2)$ for any y_1 and y_2 s.t. $p(y_1) > 0$ and $p(y_2) > 0$. This means $\hat{s}_{mmse}(y)$ is an increasing function for values of y s.t. $p(y) > 0$. □

Since the conditional mean preserves the rank of the attacked image pixel values, we use the conditional mean to evaluate images that go through a point operation. From the histogram $h(s, y)$ of pixel values, we can approximate the conditional mean as follows:

$$\begin{aligned}\hat{s}_{mmse}(s) &= \sum_s sp(s|y) \\ &\approx \frac{\sum_s sh(s,y)}{\sum_s h(s,y)}.\end{aligned}$$

2.2. Compensating for Pixel Loss Attacks

We define pixel loss attacks as attacks that lose the value of a pixel. Pixel loss attacks include cropping, random column and row removal. Pixel loss attacks can be seen as a packet loss due the error occurring in the channel [21–23]. Although we could use conditional mean for the lost pixels by mapping the lost pixels to an arbitrary pixel value (e.g. -1 or 256), we are ignoring the correlation between adjacent pixels in an image. The human visual system can estimate the values of lost pixels by the pixels close to the lost pixel. For pixel loss attacks, there are error concealment methods already developed [24]. Here we use the neighborhood mean for error concealment to estimate the lost pixel values as shown in Figure 3.

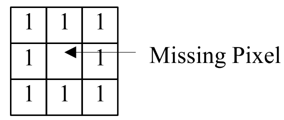

Figure 3. Neighborhood mean.

2.3. Compensation for Geometrical Attacks

A geometric attack is defined by a spatial transformation [25]. It can be expressed as

$$[x, y] = [X(u, v)Y(u, v)]$$

or

$$[u, v] = [U(x, y)V(x, y)]$$

where [u,v] is the input image coordinates and [x,y] is the output image coordinates of the spatial transformation. X and Y are the forward mapping and U and V are the inverse mapping. Inverse mapping is more common than the forward mapping in spatial transformation implementations [25] and is used in StirMark 4.0. Currently, two methods exist to evaluate geometrically attacked images [12]. One is to do a subjective evaluation. The other is to use a registration technique to match the host image and the attacked image geometrically.

As mentioned above, we take the approach of compensating the attacked image and measure fidelity in terms of MSE. For all geometric attacks in StirMark 4.0, we can obtain the exact expression for forward mapping except the local random bending attack. This eliminates the image registration step. The reason that there is no exact expression for the forward mapping in local random bending is that there are random components in the inverse mapping. For interpolation of pixels, we use the biquadratic interpolation used in StirMark 4.0. Its speed and interpolation quality is between bilinear interpolation and bicubic interpolation [26].

2.3.1. Forward Mapping for the Affine Transform

For an affine transform inverse mapping

$$\begin{aligned} u &= a_1 x + a_2 y + a_3 \\ v &= a_4 x + a_5 y + a_6 \end{aligned}$$

, the forward mapping is

$$\begin{aligned} x &= \frac{a_5(u - a_3) - a_2(v - a_6)}{a_1 a_5 - a_2 a_4} \\ y &= \frac{-a_4(u - a_3) + a_1(v - a_6)}{a_1 a_5 - a_2 a_4}. \end{aligned}$$

2.3.2. Inverse Mapping Approximation using the Bilinear Transform

We approximate the inverse mapping for the local bending attack as a piecewise bilinear transform [25] by dividing the output image into square grids.

Given four points on a square grid (x_0, y_0), $(x_0 + 1, y + 1)$, $(x_0 + 1, y_0 + 1)$, and its corresponding bilinear transformed points (u_1, v_1), (u_2, v_2), (u_3, v_3), and (u_4, v_4), we can obtain the bilinear transform as follows:

$$\begin{aligned} u &= a_1(x - x_0) + a_2(y - y_0) + a_3(x - x_0)(y - y_0) + u_1 \\ v &= a_5(x - x_0) + a_6(y - y_0) + a_7(x - x_0)(y - y_0) + v_1. \end{aligned}$$

$$
\begin{aligned}
a_1 &= u_2 - u_1 \\
a_5 &= v_2 - v_1 \\
a_2 &= u_3 - u_1 \\
a_6 &= v_3 - v_1 \\
a_3 &= u_4 - a_1 - a_2 - u_1 \\
a_7 &= v_4 - a_5 - a_6 - v_1
\end{aligned}
$$

A property of the bilinear transform is that it maps horizontal or vertical lines to straight lines in the transformed coordinates [25]. This means that a grid square in the output image coordinates is mapped to a quadrangle in the input image coordinates.

2.3.3. Forward Mapping using the Inverse Mapping Approximation

We approximate the forward mapping given the piecewise bilinear transform using a minimization algorithm [27] to find the inverse with the following cost function and its gradient:

$$f(x, y) = (U(x, y) - u)^2 + (V(x, y) - v)^2$$

$$\nabla f(x, y) = 2 \begin{bmatrix} (U(x, y) - u)(a_1 + a_3(y - y_0)) + (V(x, y) - v)(a_2 + a_3(x - x_0)) \\ (U(x, y) - u)(a_5 + a_7(y - y_0)) + (V(x, y) - v)(a_6 + a_7(x - x_0)) \end{bmatrix}$$

We used the Broyden-Fletcher-Goldfarb-Shanno (BFGS) variable metric algorithm from the gnu gsl library [28] as our minimization algorithm.

To use the BFGS algorithm, we need to choose an initial point (x_o, y_o). We make an array $\mathbf{a}_{ij}$ that stores all the initial points for the input grid points. $\mathbf{a}_{ij}$ has the same size as the input image. For each point (u, v) in the input image, we choose the initial point as $\mathbf{a}_{\lfloor u \rfloor \lfloor v \rfloor}$ and based on the value of the initial point we can determine f(x,y), and $\nabla f(x, y)$. For each output image grid square, we draw a bilinear transformed quadrangle on the vector array $\mathbf{a}_{ij}$. We use the same bilinear transform used in the inverse mapping. Quadrangles are drawn using the midpoint line algorithm [29]. The values of the quadrangle we draw with are the center point of the output image grid square which is a vector not a scalar value. To fill inside the quadrangle, we use the neighborhood mean shown in Figure 3. Using the neighborhood mean, we also fill $\mathbf{a}_{ij}$'s that are not inside any quadrangle generated by the output image grid squares.

2.4. Experimental Results

The histogram equalization image and its conditional mean image are shown in Figure 4. The amplitude scaled image and its conditional mean image are shown in Figure 5. The difference image is the difference between the attacked image and the conditional mean image. As we can see from the test images, the conditional mean did not considerably change the PSNR values for attacks that are not valumetric attacks. This may be due to the fact that the three attacks locally preserve DC values. We can see that for attacks other than valumetric attacks, conditional mean image show artifacts in the image. This is because the conditional mean does not consider the relationship between adjacent pixels or the frequency response of the human visual system.

PSNR values using conditional mean or error concealment is shown in Figure 6 and Figure 7 for cropping and row and column removal (jitter attack). We can see that the PSNR for the conditional mean images are similar for the two attacks. This is because we are losing similar amount of pixels. From comparing the two images, error concealment works better for the "0115" test image. If we compare cropping and jitter attack, jitter attack has better PSNR because interpolation is more accurate than extrapolation. If we compare the two images for the cropping attack, PSNR for the conditional mean image is better than the error concealment image for the "fcc-door" test image. This is due to the frame around the "fcc-door" test image. Results for 45 degree is shown in Figure 8. Results for a local random bending attack is shown in Figure 9. We can see that local random bending attack includes pixel loss attack due to cropping. Because of iteration in the forward mapping approximation, compensating local random bending attack takes about 5 seconds on a Xeon 3.6 GHz computer for a 600x400 image.

PSNR 17.5dB | PSNR 54.7dB
(a) Attacked image | (b) Conditional mean

Figure 4. Histogram Equalization.

PSNR 12.4dB | PSNR 52.1dB
(a) Attacked image | (b) Conditional mean

Figure 5. Amplitude Scaling with factor $\frac{9}{16}$.

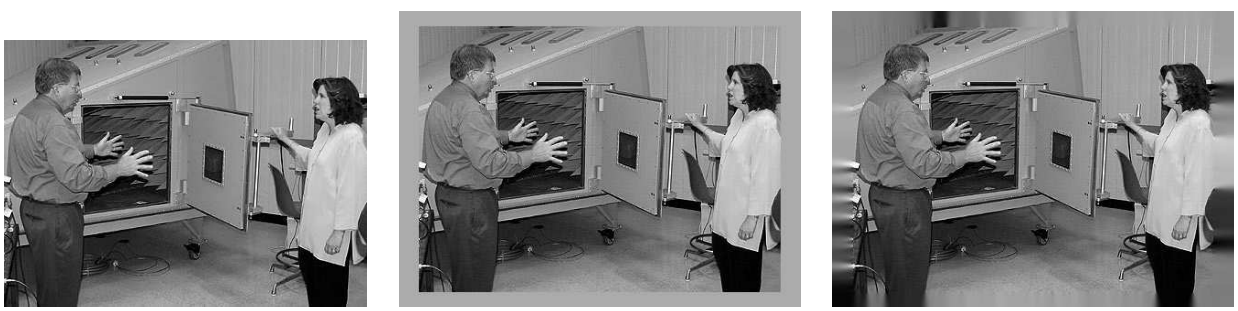

PSNR 19.4dB | PSNR 16.8dB

PSNR 22.4dB | PSNR 32.6dB

(a) Attacked image | (b) Conditional mean | (c) Error concealment

Figure 6. Cropping with factor 0.9

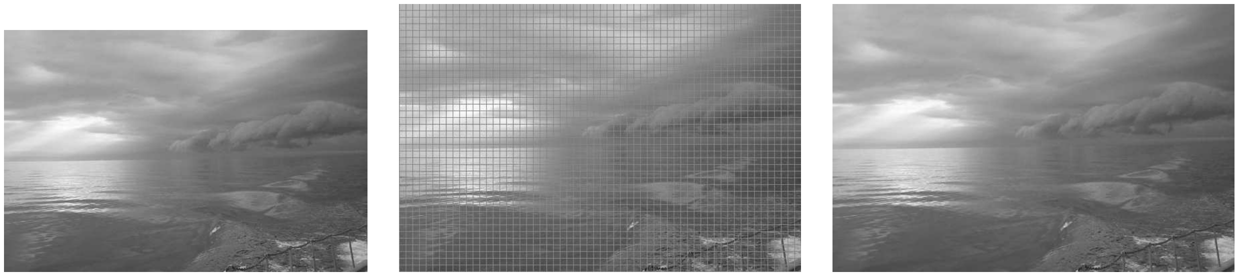

PSNR 22.9dB PSNR 41.5dB

(a) Attacked image (b) Conditional mean (c) Error concealment

Figure 7. Remove every 10th row and column.

PSNR 32.1dB PSNR 32.1dB

(a) Attacked image (b) Conditional mean (c) Error concealment

Figure 8. Rotation 45 degree.

3. RELIABILITY TESTING

Most of the watermark evaluation methods [4,5,8,12,14] fit the reliability testing framework. We define reliability as the probability that a watermarking algorithm will correctly detect or decode a watermark for a specified fidelity requirement under a given set of attacks and images. In reliability testing, a system is evaluated in terms of quality, load, capacity and performance [18]. We define quality as the fidelity of watermarked images produced by an watermarking algorithm and attacks. In this paper, we will measure fidelity using the compensated MSE described in section 2. We define capacity as the maximum data payload or minimum embedding strength that satisfies a certain error criteria. Then, we define load to be the actual embedding strength and data payload of a watermark. Because, capacity usually exceeds watermarking requirements, we will not consider capacity in this paper. The environment we used in this paper is as follows. We use PSNR as our fidelity measure and ROC and BER as our performance measure. We use the Taguchi loss function to summarize BER and PSNR results [13,14] and AUC to summarize ROC results. AUC is an estimate of the probability that the detection statistic from an watermarked image will be greater than the detection statistic from an unwatermarked image [30].

3.1. Watermark Evaluation Parameters

For our watermark evaluation parameters, we follow the evaluation parameters described in [14]. We selected ASSW, ISSW, and MSSW described in [13,14] as our test algorithms. We modified the algorithms so that it only embeds on the DCT coefficients shown in Figure 10 to reduce the visibility of watermarks [31,32]. We set the lower specification limit for PSNR$'$ [14] as 45dB. We chose the data payload to be 16 bits. This specification can be used as a specification for "fingerprinting" applications [33,34]. We tested 20 keys for no attacks and 2 keys

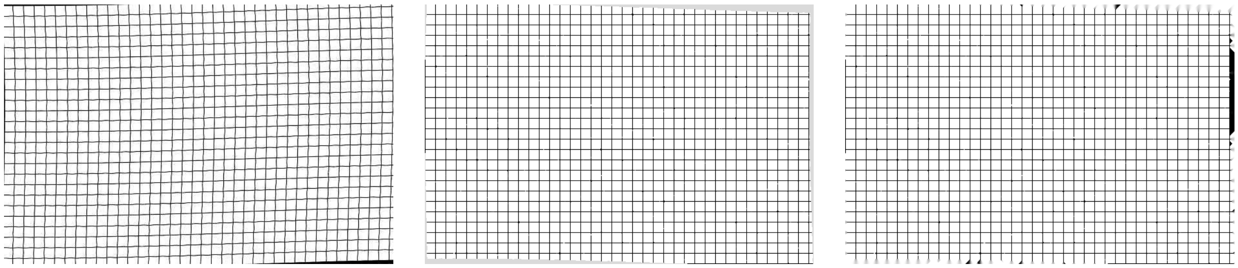

PSNR=7.4dB | PSNR=23.6 dB | PSNR=21.1dB

PSNR=24.8dB | PSNR=30.9dB | PSNR=41.2dB

(a) Attacked image | (b) Conditional mean | (c) Error concealment

Figure 9. StirMark attack

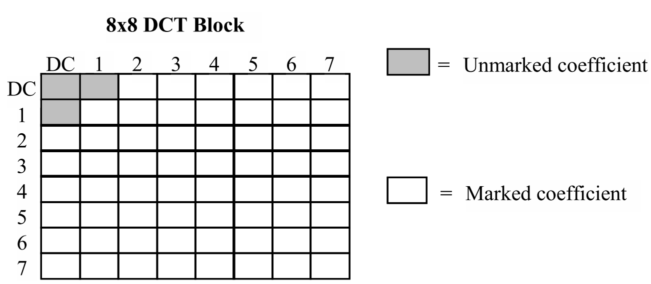

Figure 10. Watermarking in the DCT domain.

Name	No Attack	Gaussian Filtering	Sharpening
ASSW	(45.0,45.0)	(31.6,33.5)	(21.9,22.8)
MSSW	(45.0,∞)	(31.6,33.5)	(22.5,23.8)
ISSW	(45.0,45.0)	(31.6,33.5)	(21.9,22.8)

Name	JPEG	Amplitude Scaling	Histogram Equalization
ASSW	(39.0,39.8)	(12.4,13.3)	(13.3,16.1)
MSSW	(38.1,38.9)	(12.4,13.3)	(13.0,16.3)
ISSW	(39.0,39.8)	(12.4,13.3)	(13.3,16.1)

Table 1. ($PSNR'$, Average($PSNR$)) pair for different attacks

for other attacks for each image. For the image test set, we used the WET(watermark evaluation testbed) [13] image database. It has 1301 images. We choose the attacks described in [14] which include blur, sharpening, JPEG, amplitude scaling, histogram equalization. We use StirMark 4.0 [6, 7] implementation of these attacks except histogram equalization which is an implementation of the algorithm described in [16]. We measure the fidelity of the attacked image using compensated MSE instead of conditional entropy used in [14]. Similar to [4], instead of fixing the payload and embedding strength as in [14], we varied the payload and embedding strength to better characterize the watermarking algorithm. We also varied the JPEG quality from 10%, to 90% with 20% increments.

3.2. Experimental Results

Table 1 shows the average PSNR, $PSNR'$ values. Table 2 shows results for the conditional mean image PSNR ($PSNR_{cm}$). For the histogram equalization and amplitude scaling, $PSNR_{cm}$ has a significantly larger value than PSNR. Table 3 shows the BER results for different attacks. It shows that ISSW is always better than the ASSW in terms of BER for the attacks selected except histogram equalization. MSSW is better than ISSW and ASSW for the JPEG attack. It also shows that the sharpening attack lowered BER for all algorithms even though the images are degraded more than other attacks. Table 4 shows the 1-AUC results. It shows that 1-AUC values for ASSW and ISSW are similar and MSSW is better that the other two for JPEG and Gaussian filtering. Figure 11 shows the performance results for different payload and JPEG attack. As expected, the performance decreased when payload increased. Figure 12 shows the results for different JPEG attacks. It shows that performance of MSSW does not change as much compared to other two algorithms. Figure 13 shows the results for various embedding strength. It shows that ASSW and ISSW can have better performance than MSSW by sacrificing fidelity.

4. CONCLUSION AND FUTURE WORK

Evaluating fidelity of the attacked images is important for attack development and consequently watermark development. We measured the fidelity for valumetric attacks using conditional mean, pixel loss attacks using error concealment, and geometrical attacks by inverting the attacks. We also evaluated watermarks in a reliability testing framework. We evaluated watermarks by varying the embedding strength, payload, and attacks. We used the Taguchi loss function to summarize BER and PSNR results and AUC to summarize ROC results.

For future work, to measure fidelity for valumetric attacks, we could extend conditional mean by considering the frequency component of the image or correlation between adjacent pixels. For error concealment, we could use multiresolution error concealment techniques to improve PSNR values. For forward mapping of the bilinear transform used to compensate StirMark attack, we need to improve speed of the mapping. We could use information from previous pixels to improve speed. For the watermark evaluation results, we did not include confidence level results. We need to devise a way to include confidence intervals into the evaluation results. Also, we only used PSNR as our fidelity measure and we need to investigate other objective fidelity measures [12].

Name	No Attack	Gaussian Filtering	Sharpening	JPEG	Amplitude Scaling	Histogram Equalization
ASSW	(45.5,∞)	(32.6,34.1)	(24.1,24.7)	(39.3,∞)	(44.8,∞)	(44.5,44.5)
MSSW	(45.3,∞)	(32.5,34.0)	(24.7,25.6)	(38.5,∞)	(44.3,∞)	(44.3,∞)
ISSW	(45.5,∞)	(32.6,34.1)	(24.1,24.7)	(39.3,∞)	(44.8,∞)	(44.5,44.5)

Table 2. ($PSNR'_{cm}$,Average($PSNR_{cm}$)) pair for different attacks

Name	No Attack	Gaussian Filtering	Sharpening	JPEG	Amplitude Scaling	Histogram Equalization
ASSW	(1.8e-2,1.4e-3)	(4.9e-2,1.1-e2)	(1.3e-2,4.8e-4)	(7.6e-2,2.4e-2)	(2.2e-2,2.0e-3)	(1.2e-3,2.4e-5)
MSSW	(3.3e-2,4.3e-3)	(9.6e-2,4.2e-2)	(3.3e-2,4.4e-3)	(5.1e-2,1.2e-2)	(3.3e-2,4.3e-3)	(3.2e-2,3.3e-3)
ISSW	(8.1e-3,2.8e-4)	(3.9e-2,6.7e-3)	(1.3e-2,4.6e-4)	(6.4e-2,1.7e-2)	(1.1e-2,4.6e-4)	(9.7e-2,4.6e-4)

Table 3. (BER', Average(BER)) pair for different attacks

Name	Different Key	No Attack	Gaussian Filtering	Sharpening	JPEG	Amplitude Scaling	Histogram Equalization
ASSW	1.01e-3	1.09e-3	2.67e-2	1.33e-7	5.90e-2	3.64e-3	2.82e-5
MSSW	3.19e-3	3.24e-3	6.24e-3	1.12e-3	8.44e-3	3.70e-3	6.47e-3
ISSW	1.01e-3	1.11e-3	2.71e-2	4.28e-7	6.06e-2	3.68e-3	2.96e-5

Table 4. 1-AUC for different attacks

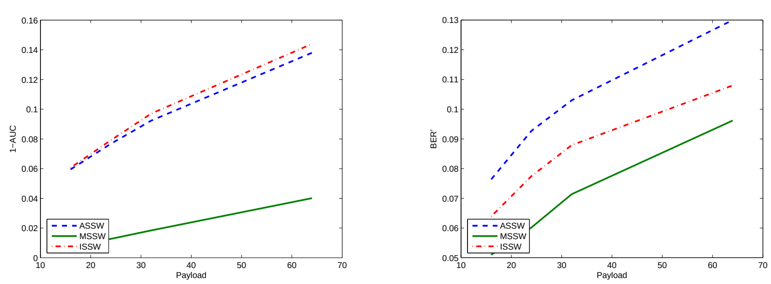

1-AUC $\quad$ BER'

Figure 11. Performance evaluation for different payloads for JPEG attack(Q=70).

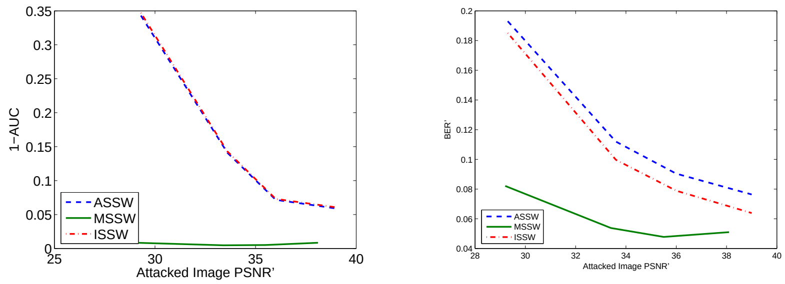

1-AUC $\qquad$ BER'

Figure 12. Performance evaluation for different JPEG attacks.

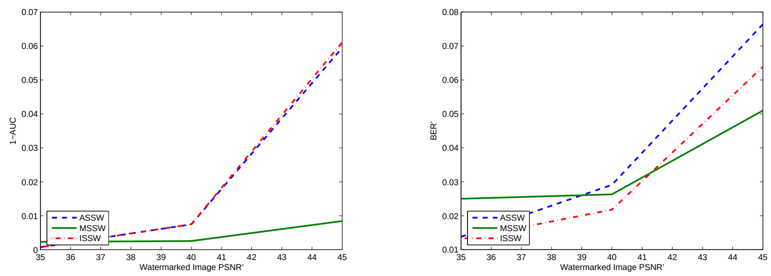

1-AUC $\qquad$ BER'

Figure 13. Performance evaluation for JPEG attack(Q=70) with different embedding strength.

REFERENCES

1. I. Cox, M. Miller, and J. Bloom, *Digital Watermarking*. Morgan Kaufmann, 2001.
2. R. B. Wolfgang, C. I. Podilchuk, and E. J. Delp, “Perceptual watermarks for digital images and video,” *Proceedings of the IEEE*, vol. 87, no. 7, pp. 1108–1126, Jul. 1999.
3. E. T. Lin, A. M. Eskicioglu, R. L. Lagendijk, and E. J. Delp, “Advances in digital video content protection,” *Proceedings of the IEEE*, vol. 93, no. 1, pp. 171–183, January 2005.
4. M. Kutter and F. A. P. Petitcolas, “Fair evaluation methods for image watermarking systems,” *Journal of Electronic Imaging*, vol. 9, no. 4, pp. 445–455, Oct. 2000.
5. J. Fridrich and M. Goljan, “Comparing robustness of watermarking techniques,” *Proceedings of the SPIE/IS&T Conference on Security and Watermarking of Multimedia Contents*, vol. 3657, San Jose, CA, Jan. 1999, pp. 214–225.
6. F. A. P. Petitcolas, R. J. Anderson, and M. G. Kuhn, “Attacks on copyright marking systems,” *Information Hiding, Second International Workshop*. Portland, OR: Springer-Verlag, Apr. 1998, pp. 219–239.
7. F. A. P. Petitcolas, “Watermarking schemes evaluation,” *IEEE Signal Processing Magazine*, vol. 17, no. 5, pp. 58–64, Sep. 2000.
8. S. Pereira, S. Voloshynovskiy, M. Madueño, S. Marchand-Maillet, and T. Pun, “Second generation benchmarking and application oriented evaluation,” *Information Hiding Workshop*, Pittsburgh, PA, Apr. 2001.
9. J. C. Vorbruggen and F. Cayre, “The Certimark benchmark: architecture and future perspectives,” *IEEE International Conference on Multimedia and Expo*, vol. 2, Lausanne, Switzerland, Aug. 2002, pp. 485–488.
10. “http://www.certimark.org.”
11. V. Solachidis, A. Tefas, N. Nikolaidis, S. Tsekeridou, A. Nikolaidis, and P. Pitas, “A benchmarking protocol for watermarking methods,” *Proceedings of the IEEE International Conference on Image Processing*, vol. 3, Thessaloniki, Greece, Oct. 2001, pp. 1023–1026.

12. B. Macq, J. Dittmann, and E. J. Delp, "Benchmarking of image watermarking algorithms for digital rights management," *Proceedings of the IEEE*, vol. 92, no. 6, pp. 971–984, June 2004.
13. H. C. Kim, H. Ogunleye, O. Guitart, and E. J. Delp, "The Watermark Evaluation Testbed (WET)," *Proceedings of the SPIE/IS&T Conference on Security and Watermarking of Multimedia Contents*, ser. Proceedings of SPIE Electronic Imaging, San Jose, CA, Jan. 2004, pp. 236–247.
14. H. C. Kim, E. T. Lin, O. Guitart, and E. J. Delp, "Further progress in Watermark Evaluation Testbed (WET)," *Proceedings of the SPIE/IS&T Conference on Security and Watermarking of Multimedia Contents*, ser. Proceedings of SPIE Electronic Imaging, San Jose, CA, Jan. 2005, pp. 241–251.
15. C. I. Podilchuk and E. J. Delp, "Digital watermarking: Algorithms and applications," *IEEE Signal Processing Magazine*, vol. 18, no. 4, pp. 33–46, Jul. 2001.
16. A. K. Jain, *Fundamentals of digital image processing*. Englewood Cliffs, NJ: Prentice-Hall, Inc., 1989.
17. A. M. Eskicioglu and E. J. Delp, "An overview of multimedia content protection in consumer electronics devices," *Signal Processing: Image Communication*, vol. 16, pp. 681–699, 2001.
18. E. E. Lewis, *Introduction to Reliability Engineering*. John Wiley and Sons, Inc., 1996.
19. P. Bas, "A quantization watermarking technique robust to linear and non-linear valumetric distortions using a fractal set of floating quantizers," *Information Hiding Workshop*, Barcelonna, Spain, May 2005.
20. P. Moulin and R. Koetter, "Data-hiding codes," *to appear in Proceedings IEEE*, December 2005.
21. E. T. Lin, C. I. Podilchuk, T. Kalker, and E. J. Delp, "Streaming video and rate scalable compression: What are the challenges for watermarking?" *Journal of Electronic Imaging*, vol. 13, no. 1, pp. 198–205, Jan. 2004.
22. A. M. Eskicioglu, J. Town, and E. J. Delp, "Security of digital entertainment content from creation to consumption," *Signal Processing: Image Communication*, vol. 18, pp. 237–262, 2003.
23. E. T. Lin and E. J. Delp, "Temporal synchronization in video watermarking," *IEEE Transactions on Signal Processing*, vol. 52, no. 10, pp. 3007–3022, Oct. 2004.
24. P. Salama, N. B. Shroff, and E. J. Delp, "Error concealment in encoded video streams," *Signal Recovery Techniques for Image and Video Compression and Transmission*. Kluwer Academic Publishers, 1998, pp. 199–233.
25. G. Wolberg, *Digital Image Warping*. Los Alamitos, CA: IEEE Computer Society Press, 1990.
26. N. A. Dodgson, "Quadratic interpolation for image resampling," *IEEE Transactions on Image Processing*, vol. 6, no. 9, 1997.
27. W. H. Press, B. P. Flannery, S. A. Teukolsky, and W. T. Vetterling, *Numerical Recipes: The Art of Scientific Computing*, 2nd ed. Cambridge (UK) and New York: Cambridge University Press, 1992.
28. "http://www.gnu.org/software/gsl/."
29. J. D. Foley, A. van Dam, S. K. Feiner, and J. F. Hughes, *Computer graphics: principles and practice (2nd ed.)*. Boston, MA, USA: Addison-Wesley Longman Publishing Co., Inc., 1990.
30. T. Fawcett, "Roc graphs: Notes and practical considerations for data mining researchers," *Technical Report HPL-2003-4, HP Labs*, 2003.
31. M. Barni and F. Bartolini, *Watermarking Systems Engineering*. Marcel Dekker, Inc., 2004.
32. M. Barni, C. I. Podilchuk, F. Bartolini, and E. J. Delp, "Watermark embedding: Hiding a signal within a cover image," *IEEE Communications Magazine*, vol. 39, no. 8, pp. 102–108, Aug. 2001.
33. *Deliverables D21: Watermarking applications and requirements for benchmarking*. The Certimark Consortium, Oct. 2000, Available from http://www.certimark.org.
34. E. J. Delp, "Is your document safe: An overview of document and print security," presented at NIP18: International Conference on Digital Printing Technologies, San Diego, CA, Sep. 29–Oct. 4 2002.